Eur. Phys. J. B **10**, 277–286 (1999)

THE EUROPEAN PHYSICAL JOURNAL B

EDP Sciences

Dynamics of sorbitol and maltitol over a wide time-temperature range

A. Faivre[1,3,a], G. Niquet[2], M. Maglione[2], J. Fornazero[3], J.F. Jal[3], and L. David[1]

[1] Groupe d'Études de Métallurgie Physique et de Physique des Matériaux[b], Institut National des Sciences Appliquées de Lyon, 69621 Villeurbanne Cedex, France
[2] Laboratoire de Physique[c], Université de Bourgogne, 21011 Dijon Cedex, France
[3] Département de Physique des Matériaux[d], Université Claude Bernard - Lyon 1, 69622 Villeurbanne Cedex, France

Received 20 May 1998

Abstract. The relaxation behaviour of two molecular glass-forming systems, namely sorbitol and maltitol, are investigated in the large temperature range relevant to the glass-transition. These data are obtained by combining three techniques, *i.e.* low-frequency mechanical spectroscopy, medium and high frequency dielectric spectroscopy, and viscosity measurements. This procedure allows to determine the relaxation map of these polyols on a wide time range [10^{-9}–10^{7} s]. Two different relaxation processes can be observed. The principal α-relaxation process exhibits a complex behaviour, comprising a non-Arrhenius temperature dependence above T_g (supercooled liquid state), and an Arrhenius behaviour below T_g (glassy state). A secondary β-relaxation is observed at higher frequencies with an Arrhenius temperature dependence. The secondary process appears in the same time-temperature range in both polyols. Consequently the molecular root of this relaxation is most likely the same in these complementary chemical systems. On the other hand, the time scale on which the α and β processes cross is very different for these two polyols. We relate this feature to the differences in the relative contributions of intra and inter-molecular interactions due to the different chemical architecture of these polyols.

PACS. 64.70.Pf Glass transitions – 62.40.+i Anelasticity, internal friction, stress relaxation, and mechanical resonances – 77.22.Gm Dielectric loss and relaxation

1 Introduction

The relaxational behaviour associated with the glass transition is known to be complex [1].

(i) The main α-relaxation process covers a wide range of time scale, requiring the use of several probes to characterise it. The relaxation spectra obtained, for example, by dielectric, mechanical, NMR spectroscopies, or by various scattering techniques, are usually wider than a Debye spectrum, and the relaxational functions are clearly non-exponential. A great number of theoretical approaches [2–7] have been proposed in literature to understand these striking features and to give some physical meaning to the empirical functions used to fit experimental data. To explain the fact that the dynamics of the α-relaxation cannot be rationalised within the simple picture of thermal activation over a well defined barrier, the idea of cooperativity in the motions of molecules, in the glass transition range, has been proposed for a long time [1]. However, there is still no clear agreement about the precise molecular nature of these cooperative motions and their relation to the microstructure.

(ii) In addition to the above process, a secondary or β-relaxation process is often observed at higher frequency. This secondary relaxation has been studied in various glasses [8–11] however the question of its origin is also still controversial. The Mode Coupling Theory [12] predicts the existence of an universal β-process in glass-forming liquids. But, this M.C.T. fast β-relaxation process, observed by Neutron Scattering [13] occurs on a completely different time scale, than the usual slower β-process, first described by Johari [14].

In order to improve our knowledge about the Glass Transition phenomenon, it is of great interest to collect data relevant to both of these relaxation processes, over the widest possible frequency range [15,16]. In the past, numerous experimental investigations have been performed on various kind of glass-forming systems [17], using different techniques, but generally on a limited frequency/temperature

[a] *Current address:* Laboratoire des Verres, Université Montpellier II, CC 069, 34095 Montpellier Cedex 5, France
e-mail: `alfaivre@univ-montp2.fr`
[b] UMR CNRS 5510
[c] ESA CNRS 5027
[d] UMR CNRS 5586

range. Moreover, only few data relevant to the comparison between the results obtained by different techniques exist in literature [18–21], partly because the experiments are usually performed on slightly different samples, and because the frequency-range where techniques overlap is often small.

In this work, we choose to study two simple and complementary molecular glass-forming systems, namely sorbitol and maltitol. We determine the relaxation behaviour of those polyols on a wide time-temperature range, combining three macroscopic techniques: low-frequency mechanical spectroscopy, dielectric spectroscopy and viscosity measurements. The data are analysed in the framework of a model [7,22,37], with parameters related to molecular features of glass-forming systems, and taking into account the cooperative features of the glass transition.

2 Experimental approach

2.1 Materials

D-sorbitol (biochemical grade) was purchased from *Merk* (Ref. 7759). Maltitol is a commercial product from *Roquette S.A.* company (Lestrem). The chemical formulas of these products are given in Figure 1.

Crystalline powders of these products were heated above their melting temperature T_{f}, respectively at 453 K for maltitol and 420 K for sorbitol, for 15 minutes and then cooled down to obtain glassy samples. This treatment was performed under vacuum in order to prevent the samples from moisture absorption. Care was also taken to avoid thermal degradation. The glass transition temperature T_{g} of these molecular systems are respectively 273 K for sorbitol [23] and 323 K for maltitol [24], as measured by DSC at a heating rate of 3 K/min. The higher value of T_{g} for maltitol can be related to the more complex structure of this polyol. The ratio $T_{\mathrm{g}}/T_{\mathrm{f}}$ is respectively of 0.73 for sorbitol and 0.77 for maltitol.

2.2 Experimental techniques

Low frequency dynamic mechanical spectrometry measurements were performed with a inverted torsional pendulum, working in forced oscillation mode [25]. It allows the determination of the dynamic modulus $G^* = G' + iG''$ in the temperature/frequency window: [100 K–400 K]/[1 Hz–10^{-4} Hz], in helium atmosphere. sorbitol forms a glass below room temperature, preventing the obtaining of bulky samples which could be analysed directly. Consequently, a special experimental procedure was used to study this sample, and is described elsewhere [26].

Combining the use of two setups [27], impedance spectroscopy measurements allowed the determination of the dynamic dielectric modulus $M^* = M' + iM''$, on a wide frequency range 10 Hz $< f <$ 10^9 Hz. It is worthwhile to remind that $M^* = 1/\varepsilon^*$, where ε^* is the dynamic dielectric susceptibility. At low frequency (10 Hz $< f <$ 10^7 Hz), a HP 4192 A impedance analyser was used, and the highest frequency range (10^6 Hz $< f <$ 10^9 Hz) was reached using a radio frequency HP4191A analyser. The same cell with the same content was used in both the high and low frequency experiments.

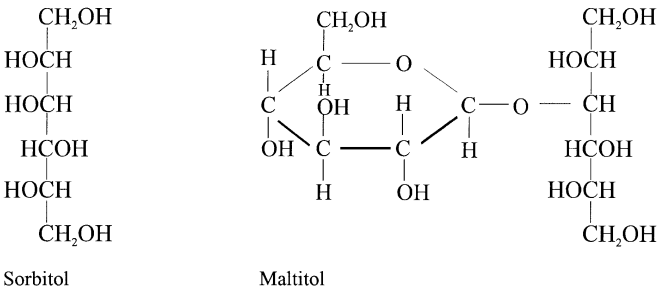

Fig. 1. Chemical structure of sorbitol and maltitol.

Viscosity measurements were carried out, using three different setups in order to cover a large temperature range (corresponding to 12 decades of viscosity). The details of these measurements are described elsewhere [28].

2.3 Determination of the relaxation times

Each spectroscopic technique is related to a particular aspect of molecular motions in the system. The problem is to compare the results issued from each of the techniques used here. They all make use of a weak perturbation (mechanical or electric field), allowing the use of the linear response theory. However, as we deal with an interacting many-body system, it is difficult to express the contribution of the various degrees of freedom. The microscopic analysis of the coupling between the perturbation and the system is therefore non-trivial. As a consequence, we start by comparing characteristic relaxation times which can be determined from each different technique. In this goal, a homogeneous treatment of the data is required.

For the viscosity data, we use the well-known Maxwell equation yielding to a relaxation time τ_η given by:

$$\tau_\eta = \frac{\eta}{G_\infty} \tag{1}$$

where η is the viscosity and G_∞ is the high frequency shear modulus. The weak evolution of G_∞ with temperature is considered to be negligible compared to the evolution of the viscosity.

From the isothermal spectra measured by mechanical frequency scans, it is possible to determine a characteristic relaxation time $\tau_{G''}$, assuming that $\omega\tau_{G''} = 1$ when $G''(\omega)$ is maximum, as proposed by the linear viscoelastic theory [29].

By analogy, the same analysis can be performed with dielectric spectra, leading to the calculation of the characteristic dielectric time $\tau_{M''}$, when $M''(\omega)$ is maximum. Dynamic results can be represented either as a susceptibility (mechanical compliance J^*, dielectric susceptibility ε^*) or as a rigidity (mechanical modulus G^*, dielectric modulus M^*), these two quantities being related to each

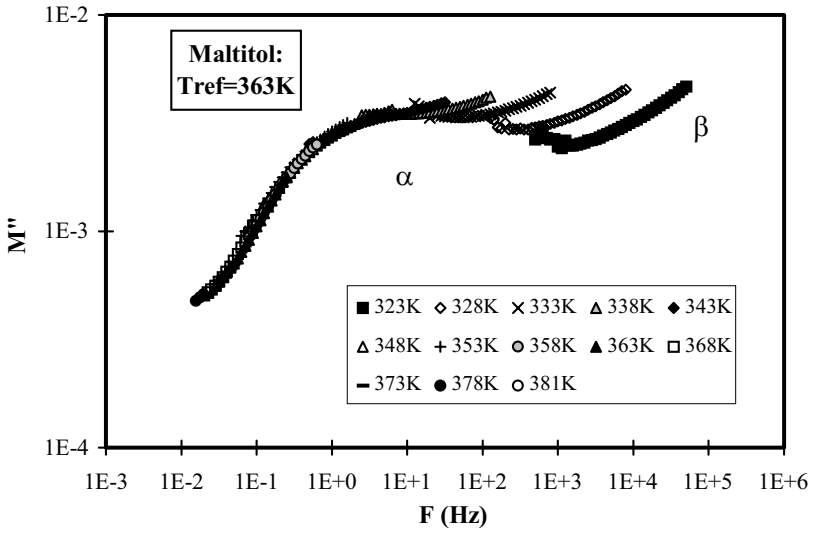

Fig. 2. Master curve of M'' at 363 K, built from the isotherms measured by dielectric spectroscopy for maltitol.

other by the following equations:

$$J^* = 1/G^* \tag{2}$$

respectively

$$\varepsilon^* = 1/M^*. \tag{3}$$

The maxima of the loss part of these complex quantities J^* (respectively ε^*) and G^* (respectively M^*), appears at significantly different frequencies. In order to quantify the mean relaxation time in an homogeneous way, we choose to use the maximum of the imaginary part of the modulus both for mechanical and dielectric data, as for viscosity measurements. This choice is some how arbitrary, also it has been discussed earlier in literature, that the use of the modulus to represent dielectric data allows to separate interfacial polarisation, from conductivity and dipolar reorientation contributions [30]. It must be quoted that the comparison between different techniques is seldom homogeneous in literature, leading to some confusion and discrepancies.

The original isotherms of G' and G'' *versus* frequency, determined by mechanical spectrometry for both maltitol and sorbitol, have been reported previously [26]. Figure 2 presents the master curve of M'' for maltitol, obtained by shifting the dielectric isotherms of M'' along the frequency axis. The observed maximum of M'' corresponds to the α-relaxation. The increase of M'' at high frequencies is related to the presence of the secondary β-relaxation. Other isotherms have been performed at lower temperatures and higher frequencies to study this secondary relaxation. The determination of the characteristic dielectric relaxation times is difficult, as α and β processes are close to each other. An interesting mathematical procedure has been proposed recently for the treatment of the dielectric data in the region where α and β processes merge [40]. Here we avoided the use of any mathematical model to analyse our data. To determine the characteristic relaxation time, we simply used the values of the shifting factor allowing to built the master curves (assuming thermorheological simplicity), when the maximum of the loss part was not clearly revealed. A similar analysis was carried out with sorbitol spectra.

3 Results

Figures 3 and 4 display the relaxation maps, *i.e.* the set of all the relaxation times τ_η, $\tau_{G''}$, $\tau_{M''}$ determined by the different techniques, respectively for sorbitol and maltitol. We can observe that these investigations reveal two general relaxation processes for both systems. The slower one, being the so-called principal or α-relaxation process, which exhibits a clearly non-Arrhenius behaviour above the glass-transition T_g. An Arrhenius behaviour is observed for temperature below T_g, when the system is out of thermodynamic equilibrium, but in a frozen structural state. An other secondary-relaxation process, often called β-process (β_slow or β-Johari) appears at higher frequencies, with an linear behaviour *versus* $1/T$.

Although there is a significant discrepancy between the relaxation times determined by the different techniques for a same relaxation process, two main α and β patterns can clearly be observed. As Figures 3 and 4 are plotted in a logarithmic scale for the time axis, the vertical shift factor between the relaxation time issued from each technique is not negligible. On the other hand, similar temperature dependence of each relaxation process can be observed for all the techniques, at least on the limited temperature range where the data overlap. This can be seen in Figure 5, where a normalized plot of the maltitol and the sorbitol data is displayed. It has been obtained by shifting the data along the logarithmic time axis by a constant value for each technique, each product, and each relaxation process. Using the mechanical data as an arbitrary reference technique, the ratio $\tau_{\mathrm{mech.\,Spectr.}}/\tau_\eta$ and $\tau_{\mathrm{mech.\,Spectr.}}/\tau_{\mathrm{dielect.\,Spectr.}}$ were found

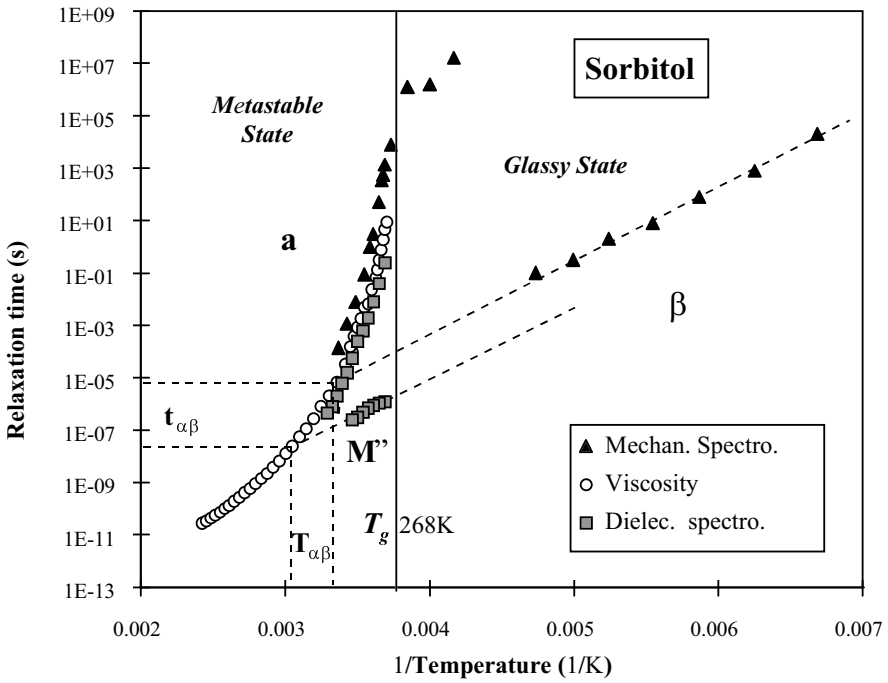

Fig. 3. Characteristic relaxation times deduced from dynamic mechanical, dielectric and viscosity measurements for sorbitol, plotted as a function of 1/Temperature.

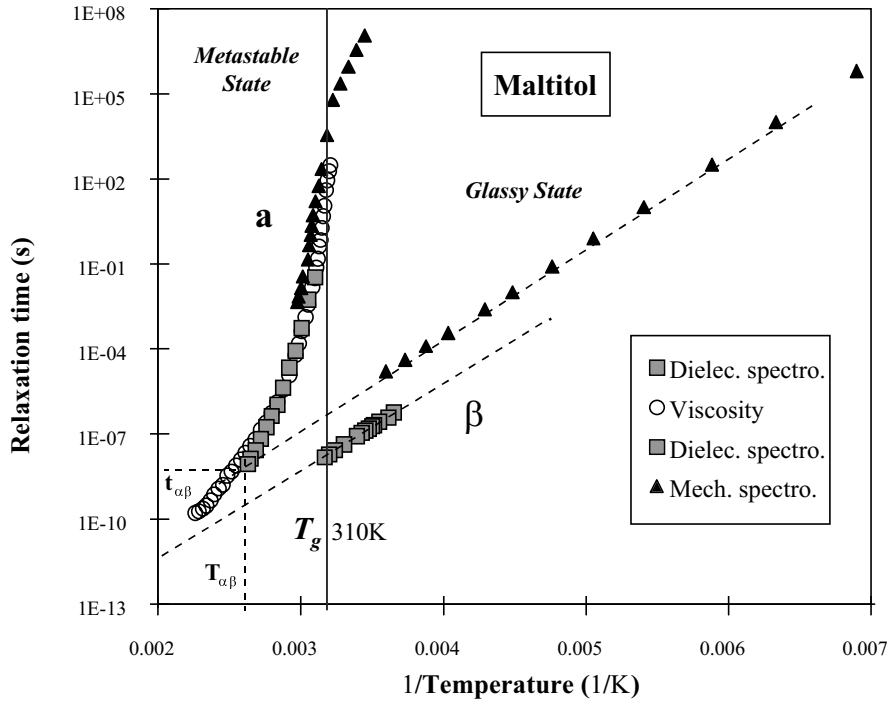

Fig. 4. Characteristic relaxation times deduced from dynamic mechanical, dielectric and viscosity measurements for maltitol, plotted as a function of 1/Temperature.

to be respectively 15 and 30, for both products and both relaxation processes. A slightly different value was obtained for the dielectric α-relaxation of sorbitol, where the ratio $\tau_{\text{mech. Spectr.}}/\tau_{\text{dielect. Spectr.}}$ is 50. The relaxation times issued from dielectric spectroscopy appear to be always smaller than those determined by mechanical measurements. These conclusions are in agreement with previous results obtained for poly(vinylethylene) [20] and for salol [21].

To go a step further, it is necessary to analyse each of the relaxation processes. We thus describe successively in

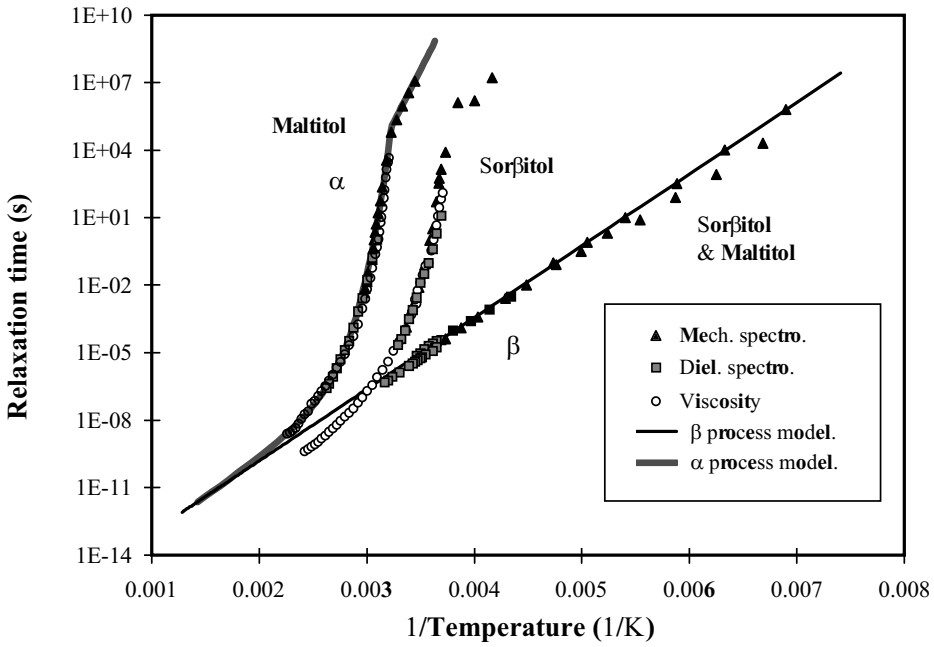

Fig. 5. Superposition of the normalised relaxation maps of sorbitol and maltitol, taking mechanical data as an arbitrary reference. The full lines correspond to the modelling of the data, using equations (7, 8, 9, 10) and the values of the parameters presented in Table 3.

Table 1. Apparent activation energies values and of the pre-exponential factors of the β-process, as determined by dielectric and mechanical data.

	Mechanical		Dielectric	
Systems	E_β (kJ/mol)	$\tau_{0\beta}$ (s)	E_β (kJ/mol)	$\tau_{0\beta}$ (s)
Sorbitol	58.6 ± 2	3×10^{-16}	61.4 ± 4	2×10^{-18}
Maltitol	61.7 ± 0.5	6.7×10^{-17}	61.3 ± 0.8	1.2×10^{-18}

more details, the β and α processes, and their cross-over region.

3.1 Secondary β-relaxation

3.1.1 Activation parameters

The relaxation time associated with the β-relaxation, either measured by mechanical or dielectric spectroscopies, shows an activated temperature dependence according to:

$$\tau_\beta = \tau_{0\beta} \exp\left(\frac{E_\beta}{RT}\right). \quad (4)$$

The apparent activation energy E_β and the pre-exponential time $\tau_{0\beta}$, as determined from mechanical and dielectric measurements are given in Table 1.

The value of the activation energy (about 61 kJ/mol) is the same for both spectroscopic techniques, and appears also to be the same for both polyols. This value is in agreement with the previous studies of Naoki [31] and Gangasharan [32] on sorbitol. On the other hand, the value of the pre-exponential factor $\tau_{0\beta}$ is more sensitive to the spectroscopic techniques. The obtained value is lower for dielectric than for mechanical measurements. Furthermore, these $\tau_{0\beta}$ values are small, both below the Debye time (10^{-14} s). It is thus difficult to analyse the motions associated with the β-process as a simple hopping process. Figure 5 shows that, beside the fact that the activation energy of the β-process is the same for sorbitol and maltitol, it occurs on the same time-temperature range, leading to the conclusion that the β-process should have the same molecular origin in both systems.

3.1.2 Amplitude of the β-process

The relative amplitude between the principal and the secondary relaxation depends on the probe used for the measurement. Figures 6 and 7 display the Cole-Cole diagrams of respectively, the mechanical and the dielectric moduli, measured for sorbitol samples. It appears clearly that the strength of the principal relaxation is higher than this of the secondary relaxation as measured by mechanical spectrometry, whereas this is the contrary, for dielectric results. Moreover in Figure 6, the amplitudes of both α and β mechanical relaxation do not evolve significantly with temperature. On the other hand, in Figure 7, a clear increase of the dielectric secondary relaxation amplitude is observed with temperature, when the amplitude of the principal process decreases with temperature. Actually, most of the isotherms were performed around or below the T_g for mechanical measurements, when they were carried out above T_g, for dielectric ones. Figure 8 shows the evolution of the maximum of M'' as a function of normalised

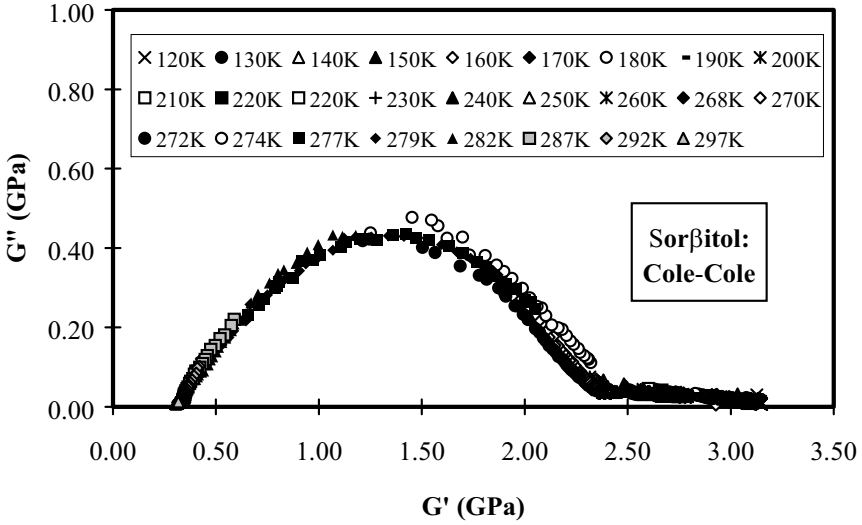

Fig. 6. Cole-Cole representation of the isothermal spectra of the shear moduli G' and G'' measured by mechanical spectroscopy, on sorbitol, for temperature ranging from 120 K to 297 K.

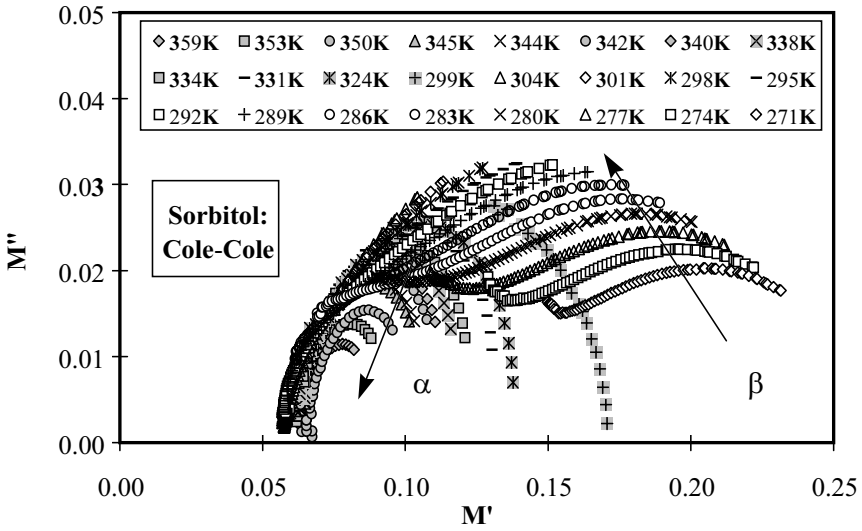

Fig. 7. Cole-Cole representation of the isothermal spectra of the moduli M' and M'' measured by dielectric spectroscopy, on sorbitol, for temperature ranging from 271 K to 359 K.

temperature T/T_g, for both sorbitol and maltitol. One can observe a small increase of the strength of M'' with temperature below T_g and a steeper one above T_g. The actual change occurs even slightly below T_g. Similar evolution have been reported for different carbohydrates [32] and polymers [33,34]. Due to the fact that it is difficult to separate the contribution of the α-relaxation process to the β-process, the trend is not straightforward to interpret. This kind of behaviour is similar to the temperature dependence of other thermodynamic and structural properties, such as the enthalpy, the specific volume [29], the density fluctuations [35]. Thus, the strength of the β-process appears to be significantly affected by the change in the density fluctuations, (*i.e.* increase of disorder and mobility), associated with the glass transition [35]. The steeper variation of the strength of the dielectric β-process above T_g can either be ascribed to an increase of the number of molecules participating to β-process, or to an increase in the dipolar moment associated with the β-process. This can be achieved either by an increase in the number or the size of the relaxation units, or by a larger charge anisotropy, when the disorder increases.

3.1.3 Conclusion

As it is the case for many glass-forming systems, the molecular origin of the β-process cannot be clearly assessed from macroscopic relaxation results. In this context further investigations by NMR spectroscopy are on going. However, two conclusions can be drawn. First, the molecular origin of the secondary relaxation appears to be similar in sorbitol and maltitol. Second, due to the low value of the pre-exponential factor, a unique and

Table 2. Values of T_g, of the apparent activation energies of the α-process E_{iso} and E_{meta}, respectively measured in the isostructural state ($T < T_g$), and in the metastable supercooled liquid state at $T = T_g$, and of fragility parameter m. The values are determined from mechanical measurements both for maltitol and sorbitol. Values of the parameters T_0, τ_0 and D, obtained by fitting the empirical V.F.T., on the normalised relaxation map of sorbitol and maltitol (Fig. 5).

Systems	T_g ($\sim 10^4$ s) (K)	E_{iso} (kJ/mol)	E_{meta} (kJ/mol)	m	D	τ_0 (s)	T_0 (K)
Sorbitol	268	192	503	225	7	10^{-13}	226
Maltitol	310	197	557	216	5.9	10^{-13}	272

Table 3. Values of the parameters used to model the normalised relaxation map the of sorbitol and maltitol, with equations (7, 8, 9, 10).

	t_0 (s)	$\tau_{0\beta}$ (s)	E_β (J/mol)	ΔH_{fd} (J/mol)	ΔS_{fd} (J/K/mol)	a	T_g (K)	$b(T_g)$
Maltitol	3×10^{-11}	6.7×10^{-17}	61 000	30 450	90	0.7	310	0.34
Sorbitol	3×10^{-9}	1×10^{-16}	61 000	27 900	92	0.8	268	0.32

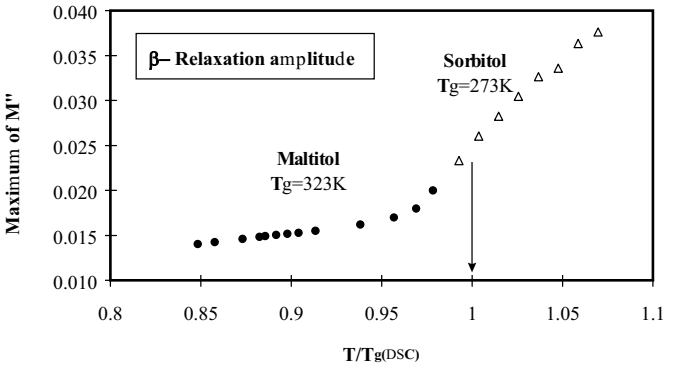

Fig. 8. Variation of the maximum of the imaginary part of the dielectric modulus, plotted as a function of temperature normalised by T_g (T/T_g), for both sorbitol and maltitol.

simple hopping motion cannot be considered as a root of the β-process, all the more as the spectra associated with this process are widely distributed. Both remarks lead to the conclusion that an important part of the β-process is probably associated to the intermolecular interactions, as can be expected in these hydrogen-bonding systems. Due to its chemical structure (see Fig. 1), maltitol should have a larger amount of intra-molecular interactions than sorbitol, as a result of interactions between the pyranic ring and the sorbitol-like chain in maltitol.

3.2 Primary α-relaxation

In Figures 3 and 4, a clear change in the dynamics of the principal α-relaxation can be observed at T_g. This glass transition temperature appears for a time scale of about 10^4 s, longer than the conventional time scale of 100 s. Indeed, in the case of these very low frequency dynamic mechanical measurements, the time needed for each frequency scan is about 12 hours, giving rise to a very large relaxation time at T_g. Physical ageing was thus performed in order to keep the system in the supercooled liquid state (thermodynamic equilibrium), for reasonable ageing time (2 days). Measurements in the glassy state were carried out by lowering the temperature enough, so that the microstructure remains frozen on the time scale of the experiment. The structural relaxation time was much longer (more than 2 days) than the time of the experiment (12 hours). The obtained glassy states were thus iso-configurational states. We can observe an Arrhenius behaviour of the α-relaxation time below T_g, and the apparent activation energy E_{iso} of these low temperature behaviour is given in Table 2. These apparent values are high and nearly the same for both polyols (~ 200 kJ/mol).

Above T_g, in the supercooled liquid state, we achieved data from the different techniques at our disposal. As for the β-process, it appears that even if each spectroscopy yields significantly different characteristic relaxation times for the main α-relaxation, the apparent activation energy is independent of the probe, at least in the range where data overlap, and in the limit of our experimental resolutions. This is shown on the normalised relaxation map of maltitol displayed in Figure 5. Moreover no clear change in the dynamic regime can be deduced at the melting temperature, or at any other particular temperature above T_g. The apparent activation energy E_{app}, as determined by $\frac{d \ln \tau_x}{d(1/RT)}$, where τ_x is τ_η, $\tau_{G''}$, or $\tau_{M''}$, merely decreases as the temperature is decreasing to T_g. The extremely high values determined in this temperature range cannot be rationalised within the simple picture of thermal activation over a well defined barrier. At very high temperature, E_{app} seems to reach a lowest constant value closed to 50 kJ/mol, yielding to an Arrhenius temperature behaviour.

The value of the apparent activation energy at T_g is directly related to the fragility parameter m, proposed by Angell [36] to classify the glass-forming liquids:

$$m = \left. \frac{d \ln(\tau)}{dT_g/T} \right|_{T=T_g} \quad (5)$$

which is also given in Table 3. It appears that both polyols have the same fragility and can be classified as fragile systems.

The temperature dependence of the α-relaxation time is often described by the empirical equation of Vogel-Fulcher and Tamman:

$$\tau_m = \tau_0 \exp\left(\frac{DT_0}{T - T_0}\right) \tag{6}$$

where D, T_0 and τ_0 are temperature independent. As each type of experiment gives rise to different relaxation times, it is not possible to determine only one set of parameters for all the three techniques. We then apply equation (6) to the normalised Arrhenius plots. The obtained values of the parameters D, T_0 and τ_0 are given in Table 2. This empirical equation allows a good description of the normalised relaxation map, but only above T_g.

3.3 Cross-over α-β

Few information have been given in literature about the cross-over between α and β relaxations, most probably because of the difficulty of separating the α and β processes in the merging region [40]. Goldstein and Johari suggested that the β-relaxation is an intrinsic property of the glassy state, due to local rearrangements in the configurational hypersurface of a glass. This interpretation leads to a tangential merging of the α and the β processes at high temperature. However our results show that, if for maltitol this assumption could be valid, for sorbitol, the linear extrapolation of β-process clearly crosses the main α-relaxation for a time scale of about 10^{-6} s (Fig. 5). A clear crossover can also be observed in other systems, like PMMA. More recently, Rössler [42] proposed that the bifurcation between both processes happens at a temperature $T_{\alpha\beta}/T_g = 1.18$–$1.28$, $T_{\alpha\beta}$ being close to the critical temperature T_c of the Mode Coupling Theory. As different relaxation times are obtained by each techniques, the cross-over occurs actually in a temperature range, rather than at a critical given temperature, when we extrapolate linearly the secondary relaxation process. This α-β cross-over would happen between 290 K and 335 K for sorbitol, and at temperature higher than 368 K for maltitol (see Figs. 3 and 4). The corresponding time range are respectively 10^{-7} to 10^{-5} s and smaller than 10^{-8} s. The ratio $T_{\alpha\beta}/T_g$ is around 1,2 for sorbitol, and 1,3 for maltitol, in agreement with typical ratio observed in fragile liquids [42].

4 Discussion

In order to give some physical meaning to these results, we attempt to model our data in the framework of a theory proposed by Perez *et al.* This model [22,37] suggests that the molecular mobility around T_g, implies *hierarchically correlated motions* of atoms in the glass transition range and leads to the following expression of the relaxation time τ_{mol}:

$$\tau_{mol} = t_0 \left(\frac{\tau_1}{t_0}\right)^{1/b} \tag{7}$$

t_0 is a scaling time parameter, τ_1 is the life time for the fastest or elementary molecular motion, which is identified with the relaxation time of the Johari's β-process: $\tau_1 = \tau_\beta$, and b gives the effectiveness of correlation effects ($0 < b < 1$).

Expression (7) is analogous to that given by the coupling model introduced by Ngai [6], but it comes from different physical arguments. The interest of the approach proposed by Perez resides in the fact that it relates the degree of cooperativity, given by b, to the concentration of density nanofluctuations in the system. In this framework these regions of high or low density, associated with high level of enthalpy, are called *quasi-point defects* (q.d.p.). As the microstructure is frozen-in at $T < T_g$, the concentration of q.d.p. and consequently b, remains constant, leading to an Arrhenius dependence of τ_{mol} *versus* temperature for the glassy state ($T < T_g$) (see Eq. (7)). On the other hand, above T_g, the increase in nanofluctuations density with temperature [41] implies that b is temperature dependent. The variation of b with temperature, above T_g, can be expressed in first approximation, as a Taylor expansion of b around $b(T_g)$, leading to:

$$b(T) = b(T_g) + a\big(C_d(T) - C_d(T_g)\big) \quad \text{for } T > T_g \tag{8}$$

where $C_d(T)$, the concentration of q.d.p. in thermodynamic equilibrium, can be determined by statistical arguments and is given by:

$$C_d(T) = \frac{1}{1 + \exp(\Delta S_f/R)\exp(-\Delta H_f/RT)} \quad \text{for } T > T_g \tag{9}$$

ΔS_f and ΔH_f are respectively increments of entropy and enthalpy associated with the formation of a q.d.p.. These values can be determined from calorimetric data [7]. Depending on the values of ΔS_f and ΔH_f, which depend on the chemical nature of the glass-forming systems, and on the value of the parameter a, the temperature dependence of b (see Eq. (8)), leads to a more or less pronounced departure from an Arrhenius behaviour of the α-relaxation process (see Eq. (7)). And this provides an interpretation for the shape of the α-relaxation process in relation with the fragility [36] of the system. The stronger the liquid is, the smaller the change in correlation effects, when temperature increases.

All the parameters used in equations (7, 8, 9, 4) can be determined from experimental data issued from calorimetric and mechanical studies, except a and t_0 which remain adjustable and are determined from the modelling of the Arrhenius diagram. Figure 5 shows the modelling obtained for the normalised map of maltitol, using in equations (7, 8, 9, 4) and the values of parameters given in Table 3. We can observe that, even if this model was first developed to interpret the mobility only in the glass transition

region, it allows the modelling of experimental results from below T_g to far above T_g.

In the case of sorbitol, the modelling using equations (7, 8, 9, 4), is not possible, because α and β relaxation curves are clearly not tangent, but cross at high temperature. The model imply that, at high temperature the correlation effects vanish corresponding to b approaching unity. Equation (7) can then simply be expressed as $\tau_{mol} = \tau_\beta$. However that is not observed experimentally for sorbitol (see Fig. 5). This clearly shows that in the case of sorbitol, the merging of α and β processes does not simply correspond to the vanishing of correlation effects leading to a simple activated process above $T_{\alpha\beta}$, as it may be suggested for maltitol.

Considering that the β-relaxation is both inter and intra-molecular in nature, we can try to analyse why the merging region is different for these two polyols. Below $T_{\alpha\beta}$, when relaxation times of the β-relaxation are shorter than τ_α, we can assume that the energy landscape of the regions related to the β-process is frozen on the time scale of the β-process. In the α and β merging region on the other hand, the time scale of the cooperative translational motions associated to the viscosity become as short as the time of the localised β-motions. This surely modifies the landscape of the β-relaxation process on the time scale of this process, specially by changing the intermolecular contributions. Due to a more complex chemical architecture, the cooperative mobility associated with the glass transition appears at higher temperatures in maltitol than in sorbitol. If the same kind of motions are involved in the β-relaxation in both polyols, the merging of α-β processes appears on a shorter time scale (higher temperature) for maltitol than for sorbitol, because the decrease of inter-molecular contribution to the activation energy of the β motions occurs at higher temperatures (higher ratio $T_{\alpha\beta}/T_g$) and for shorter time scale (lower value for $\tau_{\alpha\beta}$). The same type of analysis can be applied for other systems, like in the polymer series PMMA, PEMA, PBMA [33,34]. In these systems, the β-process occurs also on the same time/temperature range, whereas the α-process happens on different scales. Thus, the motions associated to the β-process could also have a similar molecular origin in the polyacrylates. The ratio of the intra to inter-molecular contributions of the β-process should be different for each polymers, in relation with the more and more complex chain structure, and explain the differences in the α-β crossing region. In this extended frame, it is then possible to model and understand the complete Arrhenius diagram from the glassy state up to the liquid, at temperatures above the α-β merging temperature. This can be achieved using an adequate choice of the temperature variations for the intermolecular and intramolecular contributions to the activated energy of the β-process [43].

5 Conclusion

By combining information from different spectroscopic experiments, extended relaxation map of two polyols (sorbitol and maltitol), were obtained. These results show that a significant discrepancy exists between the relaxation time issued from different spectroscopic techniques. This can be interpreted by the fact that each probe couples with different dynamic variables, and that there is no trivial interrelation among them. However the temperature dependence of the measured relaxation processes appear to be the same for all techniques, allowing the construction of normalised diagrams. The analysis of these normalised data in the framework of a model for the glass transition, yields to more physical interpretation of the mechanisms involved in the glass transition range, and more particularly, we are able to discuss the α-β cross-over on molecular level.

We would like to thank Pr. J. Perez, Dr. J. Dupuy and Pr. G. Vigier for stimulating discussions, and useful comments, and Dr. N. Nakeli for the viscosity measurements.

References

1. K.L. Ngai, G.B. Wright, *Relaxations in complex systems* (U.S. O.N.R. Arlington, VA, 1984), 309 p.
2. M.H. Cohen, D. Turnbull, J. Chem. Phys. **315**, 1164 (1959).
3. M.H. Cohen, G.S. Grest, Phys. Rev. B **203**, 1077 (1979).
4. G. Adam, J.H. Gibbs, J. Chem. Phys. **43**, 139 (1965).
5. W. Götze, L. Sjögren, Rep. Prog. Phys. **55**, 241 (1992).
6. K.L. Ngai, R.W. Rendell, A.F. Yee, Macromolecules **21**, 3396 (1988).
7. J. Perez, J. Food Eng. **22**, 89 (1994).
8. S.S.N. Murthy, J. Sobhanadri, G. Gangasharan, J. Chem. Phys. **100**, 4601 (1994).
9. R. Flores, J. Perez, Macromolecules **28**, 7171 (1995).
10. J.Y. Jho, A.F. Yee, Macromolecules **24**, 1905 (1991).
11. K. Schmidt-Rohr, A.S. Kudlik, H.W. Bekham, A. Ohlemacher, U. Pawelzik, C. Boeffel, H.W. Spiess, Macromolecules **27**, 4733 (1994).
12. W. Götze, L. Sjögren, J. Non-Cryst. Solids **131–133**, 161 (1991).
13. D. Richter, B. Frick, B. Farago, Phys. Rev. Lett. **61**, 2465 (1988).
14. J.P. Johari, M. Goldstein, J. Chem. Phys. **53**, 2372 (1970).
15. J. Colmenero, A. Arbe, A. Algeria, J. Non-Cryst. Solids **172–174**, 126 (1994).
16. F. Stickel, E.W. Fischer , R. Richter, J. Chem. Phys. **102**, 6251 (1995).
17. L. Wu, Phys. Rev. B **43**, 9906 (1991).
18. C.T. Moynihan, N. Balitactac, L. Boone, A. Litovtz, J. Chem. Phys. **55**, 3013 (1971).
19. K.L. Ngai, S. Mashimo, G. Fytas, Macromolecules **21**, 3030 (1988).
20. J. Colmenero, A. Algeria, P.G. Santangelo, K.L. Ngai, C.M. Roland, Macromolecules **27**, 407 (1994).
21. F. Stickel, E. W. Fischer , R. Richter, J. Chem. Phys. **104**, 2043 (1996).
22. J. Perez, *Physics and mechanics of amorphous polymers* (Oxford & IBH Publishing Co., New Dehli, 1998).
23. D. Simatos, G. Blond, G. Roudaut, D. Champion, J. Perez, A.L. Faivre, J. Thermal Anal. **47**, 1419 (1996).
24. M. Siniti, Ph.D. thesis, INSA de Lyon, France, 1995.

25. S. Etienne, J.Y. Cavaillé, J. Perez, R. Point, M. Salvia, Rev. Sci. Instrum. **53**, 1231 (1982).
26. A. Faivre, L. David, J. Perez, J. Phys. II France **7**, 1635 (1997).
27. M. Maglione, G. Niquet, A. Gueldry, C. Dumas, Solid State Commun. **98**, 249 (1996).
28. J. Huck, A. Nakheli, J. Phys. I France **5**, 1635 (1995).
29. J.D. Ferry, *Viscoelastic properties of polymers* (J. Wiley and Sons, New York, 1970).
30. M.G. Parthun, G.P. Johari, J. Chem. Soc. Faraday Trans. **91**, 329 (1995).
31. M. Naoki, K. Ujita, J. Chem. Phys. **99**, 6971 (1993).
32. Gangasharan, S.S.N. Murthy, J. Phys. Chem. **99**, 12349 (1995).
33. J. Heijboer, Br. Polym. J. **1**, 3 (1969).
34. J.L. Gomez-Ribelles, R. Diaz-Calleja, J. Polym. Sci. Polym. Phys. Ed. **23**, 1297 (1985).
35. A. Faivre, L. David, R. Vassoille, G. Vigier, S. Etienne, E. Geissler, Macromolecules **29**, 8387 (1996).
36. R. Böhmer, K.L. Ngai, C.A. Angell, D.J. Plazek, J. Chem. Phys. **99**, 4201 (1993).
37. J. Perez, J.Y. Cavaillé, J. Non-Cryst. Solids **172–174**, 1028 (1994).
38. P.O. Maurin, J.F. Jal, J. Dupuy-Philon, N. Asahi, J. Kawamura, T. Kamiyama, Y. Nakamura, Ber. Bunsenges. Phys. Chem. **102**, 152 (1998).
39. H.W.J. Starkweather, Macromolecules **21**, 1798 (1988).
40. A. Arbe, D. Richter, J. Colmenero, B. Farago, Phys. Rev. E **54**, 3853 (1996).
41. G. Vigier, K. Abbes, J.Y. Cavaillé, L. David, A. Faivre, J. Perez, J. Non-Cryst. Solids **235–37**, 286 (1998).
42. E. Rössler, K.-U. Hess, V.N. Noviko , J. Non-Cryst. Solids **223**, 207 (1998).
43. A. Faivre, Ph.D. thesis, INSA de Lyon, France, 1997.